Nuclear Instruments and Methods in Physics Research B 269 (2011) 1450–1454

Contents lists available at ScienceDirect

Nuclear Instruments and Methods in Physics Research B

journal homepage: www.elsevier.com/locate/nimb

Nanoscratch study of ZnO thin films deposited using radio frequency magnetron sputtering

Wei-Hung Yau [a], Pai-Chung Tseng [a], Derming Lian [b,*]

[a] Department of Mechanical Engineering, National Chung Hsing University, Taichung 40227, Taiwan, ROC
[b] Department of Mechanical Engineering, Chin-Yi University of Technology, Taichung 411, Taiwan, ROC

ARTICLE INFO

Article history:
Received 16 January 2011
Received in revised form 25 February 2011
Available online 24 March 2011

Keywords:
Zinc oxide (ZnO)
r.f. Magnetron sputtering
XRD
AFM
Nanoscratch

ABSTRACT

In this study, a radio frequency magnetron sputtering system was used to deposit zinc oxide (ZnO) thin films onto langasite substrates. The thickness of the ZnO film increased from 0.3 to 1.2 μm upon increasing the deposition power from 100 to 200 W. The predominant growth orientation was along the *c*-axis (0 0 2); the intensities of the signals in the X-ray diffraction spectrum increased significantly upon increasing the film thickness. Scanning electron microscopy images revealed columnar structures in the ZnO films and the morphology of ZnO grains is found to be continuous and dense. It is attributed that oxygen chemisorbs on the target and cases a surface layer of adsorbed oxygen. We suggest that the more neutral ion bombardment on the growing film which induces the higher sputtering rate of the growing film. From *in situ* imaging of scratched tracks, measurement of the coefficient of friction was an effective means of detecting the occurrence of structural defects in the microstructures. We also found that the chemical compositions of ZnO films prepared under various deposition powers could be investigated using X-ray photoelectron spectroscopy.

1. Introduction

Zinc oxide (ZnO) has recently emerged as a promising alternative to gallium nitride because of its large band gap and large excitation binding energy [1]. ZnO thin films are mainly used as transparent conductive films in solar cell windows. The successful fabrication of semiconductor devices incorporating ZnO will require a better understanding of its mechanical characteristics and its optical and electrical properties; indeed, contact loading during processing or packaging can significantly degrade the performance of such devices [2–4].

The mechanical properties of ZnO films have been investigated widely [5–8]. In particular, nanoscratch and nanoindentation techniques have become important tools for analyzing ZnO thin films of various compositions [9,10]. The nanoscratch technique can be used to characterize the nanotribological properties of a sample; the process involves scratching its surface with a diamond tip and recording the coefficient of friction. Although the mechanical properties of ZnO films have been discussed widely [5–11], the issue about nanotribology of ZnO films is less well understood; therefore, precise studies are required if ZnO films are to be used as structural/functional elements in devices.

In this study, the growth and characteristics of ZnO films deposited using a radio frequency (RF) magnetron sputtering system were investigated at various deposition powers. The characteristics (crystallinity, morphology, roughness, and nanotribology) of these ZnO films were measured using various techniques, including X-ray diffraction (XRD), field emission scanning electron microscopy (FESEM), atomic force microscopy (AFM), and nanoscratch techniques. The effect of the deposition power on the microstructures and nanoscratch properties was also investigated.

2. Experimental descriptions

An r.f. magnetron sputtering system using a water-cooled 4 inch-diameter Zn target (99.999%) in an Ar/O_2 gas mixture was employed to deposit ZnO films onto langasite ($La3Ga5SiO14$, LGS) substrates (substrate–target distance: 5 cm); r.f. powers of 100, 150, and 200 W were used for the deposition of three ZnO samples, respectively. In addition, the base pressure was 6×10^{-6} torr, the sputtering pressure was 3–9 mtorr, the substrate temperature was set at 200 °C, the $O_2/(Ar + O_2)$ ratio was set at 20% (purity of O_2 gas: 99.995%; purity of Ar gas: 99.995%), and the duration of the deposition was 1 h. After deposition, cross-sectional images of the ZnO films were recorded using a JEOL JSM-7001F field emission scanning electron microscope, which revealed that the thickness of the ZnO films increased regularly from 0.3 to 1.2 μm upon increasing the deposition power from 100 to 200 W. The deposition rates at 100, 150, and 200 W were, therefore, calculated to be ca. 5.0, 12, and 20 nm/min, respectively.

* Corresponding author.
E-mail address: lianderming@gmail.com (D. Lian).

0168-583X/$ - see front matter © 2011 Elsevier B.V. All rights reserved.
doi:10.1016/j.nimb.2011.03.009

To determine the morphological surface properties, the samples were scanned using a Digital Instruments Nanoscope III atomic force microscope operated at a constant scan speed (1 μm/s), with a constant load (30 nN) applied to the cantilever. The nanotribological properties of the samples were measured through nanoscratch tests, using a combination of AFM and a nanoindentation measurement system (Hysitron, Inc.), operated at a constant scan speed (2 μm/s) and constant load (5000 μN) and featuring a diamond Berkovich indenter tip (radius: 50 nm); scratching was performed at a constant scratching speed (0.13 μm/s) over a constant length (10 μm). Surface profiles before and after scratching were obtained by scanning the tip with a sufficiently small load that did not produce a measurable displacement. After scratching, the wear tracks were imaged using AFM. All tests were realized at least five times to determine the reproducibility; the data were averaged using the central regions of the scratches (i.e., neglecting any steps, peaks, or depressions that may have arisen).

3. Results and discussion

The ZnO films were polycrystalline, revealing (1 0 0), (0 0 2), and (1 0 1) peaks for hexagonal ZnO at 31.75, 34.35, and 36.31°, respectively, in their XRD spectra (Fig. 1). After deposition at 100 W, weak diffraction peaks were observed for ZnO, suggesting the onset of ZnO growth. The spectrum obtained after deposition at 150 W revealed the presence of pure and polycrystalline ZnO having a wurtzite structure [12]. The intensity of the (0 0 2) peak increased significantly upon increasing the deposition power to 200 W, revealing enhanced crystallinity in the (0 0 2) oriented plane. The average grain size in a film can be estimated using Scherrer's equation [13]:

$$D = 0.9\lambda/\beta\cos\theta$$

where D is the mean dimension of the crystallites, λ is the X-ray wavelength, and β is the full width at half-maximum (FWHM) of the (0 0 2) peak. The average grain size in the films decreased from 109 to 104 to 98 nm upon increasing the deposition power from 100 to 150 to 200 W, respectively. Lin et al. [14] reported that grain overgrowth caused by a high substrate temperature will induce a rough surface; they also suggested that the surface structure of a ZnO film is influenced by the use of zinc or oxygen support. Similar phenomena have been reported [15,16] for ZnO films deposited through dc magnetron sputtering at various temperatures, resulting in preferred orientation along the (0 0 2) plane. Thus, the average grain size is not controlled by a single parameter.

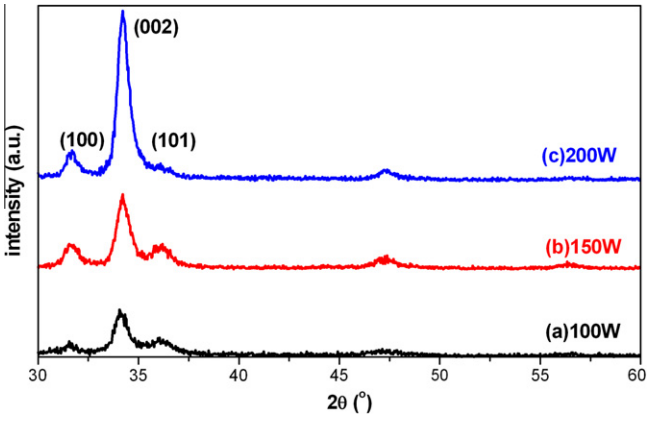

Fig. 1. XRD spectra of ZnO thin films deposited at deposition powers of (a) 100 W (weak diffraction peaks of ZnO), (b) 150 W (presence of pure and polycrystalline ZnO), and (c) 200 W (improvement of crystalline quality with power).

Fig. 2 displays SEM and AFM images representing the surface morphologies and 3D topographies of ZnO films prepared at deposition powers of 100, 150, and 200 W. It is clear that no specific epitaxial orientation occurred on the langasite substrate surface, leading to randomly oriented nuclei. The insets reveal cross-sectional SEM images of the ZnO films, the thickness of which increased regularly from 0.3 to 1.2 μm upon increasing the deposition power from 100 to 200 W. Columnar structures were observed in the ZnO films; their possible mechanism of formation has been reported previously [15,16]. The Zn and O compositions during the sputtering process were also dependent on several parameters [15–17]. Lu et al. reported [18] that the growth rates of ZnO films increase upon increasing the r.f. power and that the resulting ZnO grains were continuous and dense. In our experiments, however, the intensity of the c-axis (0 0 2) peak increased sharply upon increasing the deposition power from 100 to 200 W, while the other two peaks coexisted with much smaller intensities and greater FWHMs. Although an increased peak intensity in an X-ray diffractogram might be due to a larger thickness of the films, it might also be attributable to indirect crystallinity as a result of the higher deposition power. We suspect that under a high deposition power, more Zn atoms can reach the substrate and have more opportunity to form nuclei. In other words, more nuclei sites will be generated and a large number of small grains will grow, leading to a smaller-grain structure and a higher growth rate.

The height roughness parameter (R_a) and the root mean square roughness (R_{ms}), determined from AFM images, can be used to quantify the morphologies of ZnO films [19]. Fig. 2 provides typical images obtained using the various growth procedures; the surface roughnesses and apparent feature sizes are clearly evident. The ZnO film formed at 100 W was smooth (R_{ms} = 11.3 nm); it roughened to values of R_{ms} of 14.5 and 16.5 nm for deposition powers of 150 and 200 W, respectively; i.e., the surface roughness increased rapidly upon increasing the deposition power from 100 to 200 W. Although we obtained appropriate grain sizes and flat surface crystals, the deposition conditions affected not only the grain growth but also the Zn and O compositions during the sputtering process. When the content of supporting O atoms was increased [14], the surface morphologies of the films displayed greater roughness. Table 1 summarizes the values of R_a and R_{ms} obtained under the various growth conditions. For oxygen content in the range of 20%, rapid oxidation of the target takes place at high deposition power; this increase in secondary electron yield causes more ionization of the sputtering gas, therefore increase the sputtering rate. It is attributed that oxygen chemisorbs on the target and cases a surface layer of adsorbed oxygen. We suggest that the increased surface roughnesses based on the more neutral ion bombardment on the growing film which induces the higher sputtering rate of the growing film.

AFM studies of the scratched tracks revealed more details concerning the scratching process. Fig. 3 displays AFM images of scratched tracks formed on the ZnO/LGS samples prepared under the various deposition conditions. Fig. 3a reveals the presence of a significant creep in the ZnO film prepared at 100 W, associated with plastic deformation of the material. Under a constant normal load of 5000 μN, a plowing scratch track appeared without debris on the sides of the scratch, likely to be the cause of the lower coefficient of friction (μ = 0.1 ± 0.01). Notably, the ZnO/LGS films exhibited lower surface roughness for lower values of μ. For the ZnO film sample prepared at 150 W Fig. 3b, in addition to plowing scratch tracks, pile-up appeared on the sides of the scratches (μ = 0.175 ± 0.01). After deposition at 200 W Fig. 3c, lateral sliding emanating from the indenter edge occurred, leading to removal of the film through a ploughing mechanism; scratch debris or nanoparticles appeared inside or around the nanoscratch tracks at a

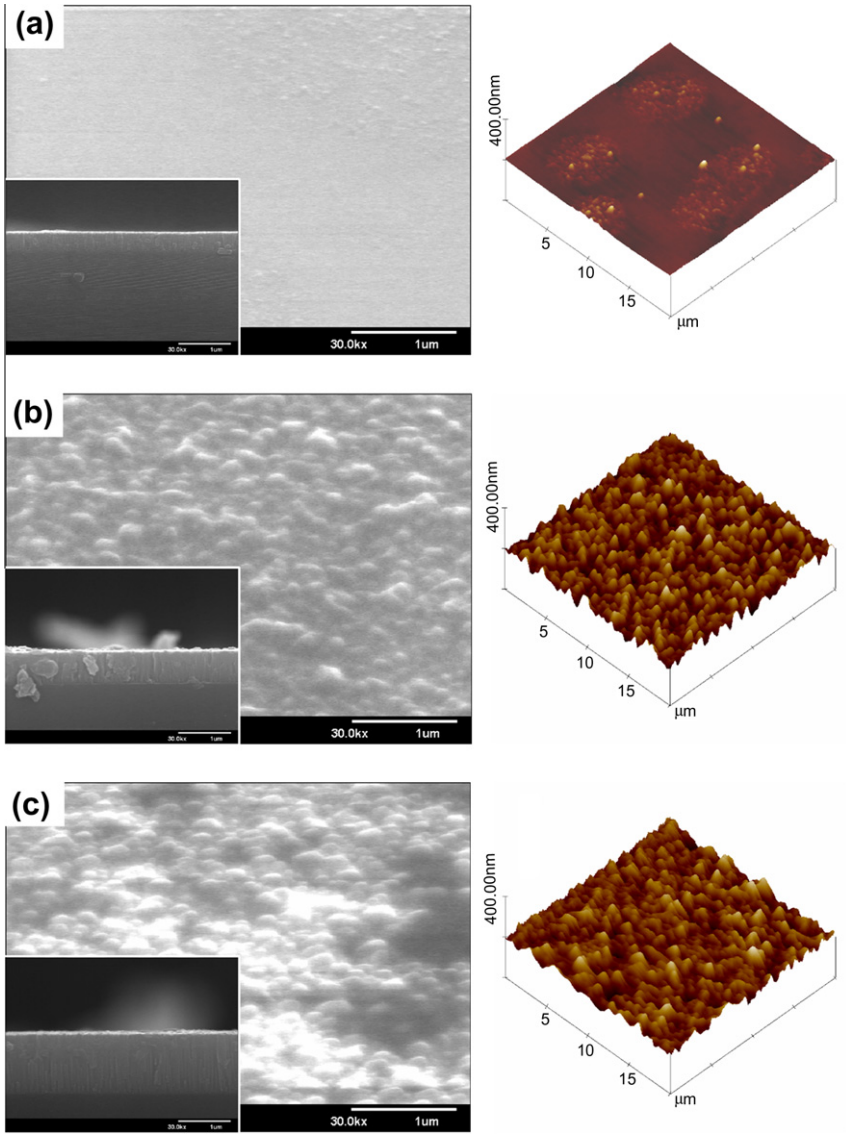

Fig. 2. SEM (inset: SEM cross-sectional images) and AFM images of the surface morphologies and 3D topographies of ZnO thin films prepared for different deposition times at deposition powers of (a) 100, (b) 150, and (c) 200 W.

Table 1
Values of Ra and Rms of ZnO films grown at deposition powers of (a) 100, (b) 150, and (c) 200 W.

Sample	Deposition power (watt)	Average roughness, R_a (nm)	Root mean square roughness, R_{ms} (nm)
(a)	100	8.6	113
(b)	150	11.4	14.5
(c)	200	13.2	16.5

higher coefficient of friction ($\mu = 0.183 \pm 0.02$). Accordingly, the plot of the load force with respect to the scratch track Fig. 3d revealed that the friction increased abruptly at a well-defined normal load of 5000 μN, resulting from interaction with the sliding stylus. The fluctuation of the friction coefficient (μ) versus scratch time (normal load) was recorded using a point-on orientation of the tip toward the layered structures of the ZnO films. In the ploughing mechanism, the contact groove zone of a brittle material is readily damaged through scratch deformation of neighboring areas. Therefore, the deposition conditions used to prepare the ZnO films affected the damage caused by the applied normal load. We suspect that ZnO films featuring smaller grains, prepared at higher growth powers, possess enhanced coefficients of friction.

In ZnO films, a columnar structure provides lower levels of friction [20]. This finding suggests that the various friction coefficients of our films resulted from variations in their crystal structures and topographies. Similar trends were reported by Lin et al. [10], who investigated the influence of the sputtering conditions on the friction coefficients of ZnO films. They found that the surface roughnesses and friction coefficients of Al-doped ZnO films increased and the (0 0 2) oriented plane was favored upon increasing the growth temperature. In addition, Jian et al. [8] reported the effect of the substrate on the surface roughness and friction coefficients of ZnO films; our ZnO/LGS samples appear to be rough and have low friction coefficients relative to those of other reported ZnO/substrate films [8]. Herein, the langasite substrate surfaces do not have a specific epitaxial orientation to follow, resulting in randomly oriented nuclei [12]. Nevertheless, the relationship between the sputtering conditions and the growth quality of ZnO film is important to study, including an investigation of their binding

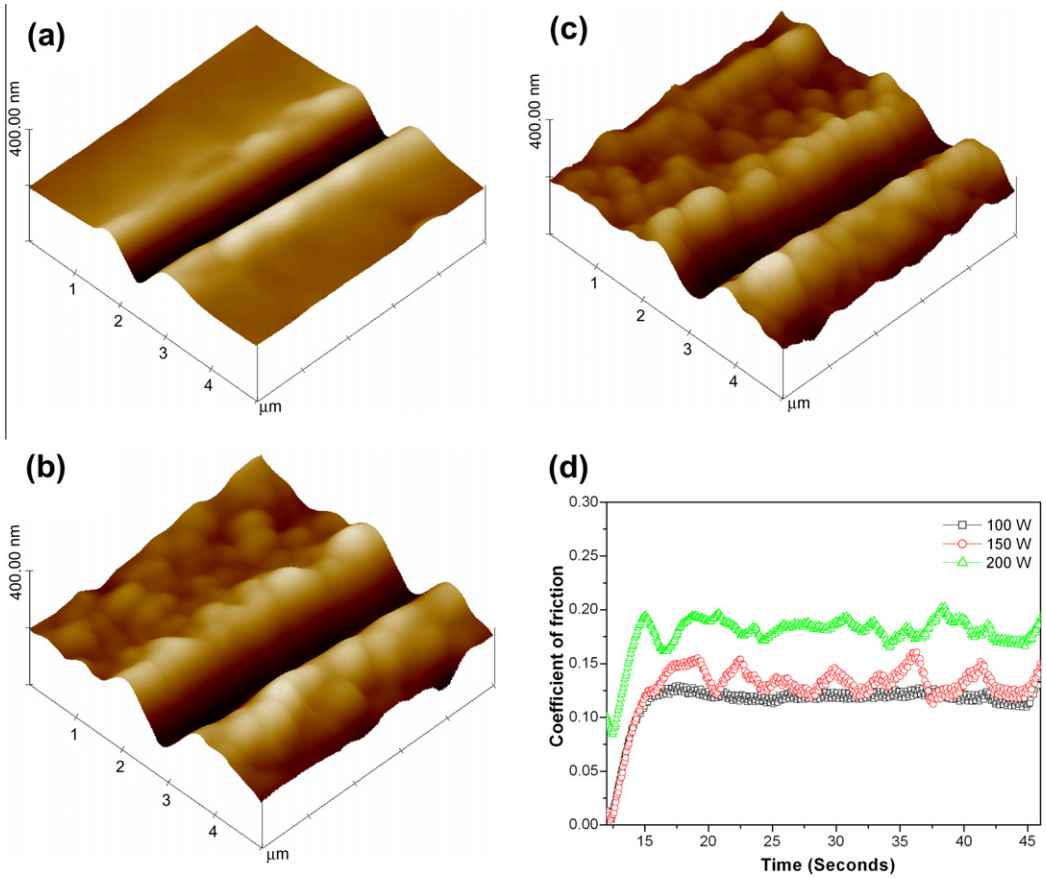

Fig. 3. (a–c) 3D AFM images of scratch tracks on ZnO/LGS samples prepared at deposition powers of (a) 100, (b) 150, and (c) 200 W. (d) Nanoscratch load plotted with respect to the coefficient of friction of ZnO thin films, at a constant normal load of 5000 μN.

energies [21,22]. It is suggested that the increase in the friction coefficient of the ZnO films was caused by not only favored grain growth along the (0 0 2) plane but also stronger Zn–O bonding when sputtering at higher deposition power.

Fig. 4 reveals that the growth power influenced the XPS data of the ZnO films. We observe that the intensity of the Zn $2p^{3/2}$ peaks increased manifestly near 1021.7 eV at deposition powers of 100 and 150 W. Furthermore, the peak then increased near 1022.5 eV

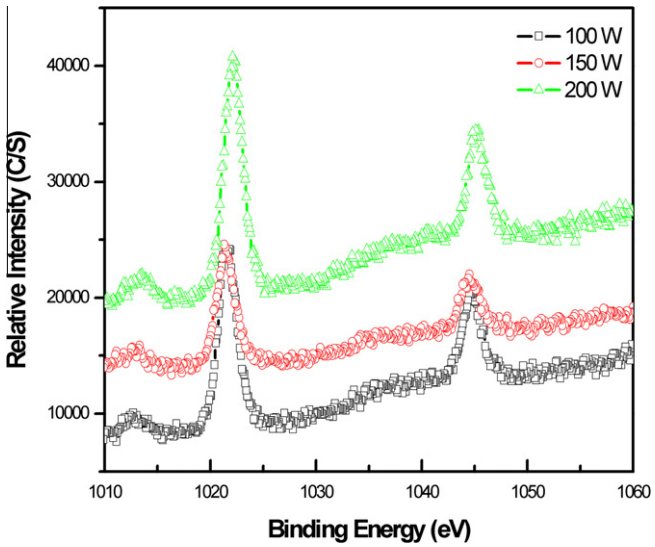

Fig. 4. Reveals the growth power influenced the XPS data of the ZnO films.

when the deposition power was 200 W, attributable to stronger Zn binding [23,24]. In Fig. 5, we attribute the binding energy of the O 1s peak at 532 eV to residual oxygen at the film surface after deposition at 100 W (e.g., O–H bonds).

In Fig. 5a, the O 1s state splits into two peaks: 529.4 eV can be attributed to the O–Zn bond formation, while the peak at 531.0 eV can be owing to the O–H bond formation. As the deposition power increased at 150 W Fig. 5b, the O 1s peak shifted to lower binding energy and a main peak emerged at ca. 530.5 eV, which we attribute to Zn–O bonds [25,26]. Therefore, it appears that Zn–O bonds became dominant during the grain growth process when deposition power increased from 100 to 200 W Fig. 5b. The XPS data suggest that the increase in the friction coefficient of the ZnO films was caused by not only favored grain growth along the (0 0 2) plane but also stronger Zn–O bonding when sputtering at higher deposition power.

In the perspective of the sputtering mechanisms, Chen et al. [9] demonstrated that an optimal oxygen content would provide ideal mechanical properties. Lee et al. [27] discussed that the plasma density, electron temperature and saturated ion current density for plasma as a function of RF input power and oxygen content. They conclude that while the RF power was increased, the plasma density and saturated ion current density increased, resulting in a decrease in electron temperature. Lu et al. [28] also mentioned that the growth rate of ZnO film increases with increasing RF power; the morphology of ZnO grains is found to be continuous and dense. From our present study, similar results for the grain size of ZnO film decreases with increasing RF power is found; therefore, it is reasonable to deduce that an appropriate amount of oxygen atoms were decomposed through reactions with the Ar plasma under the

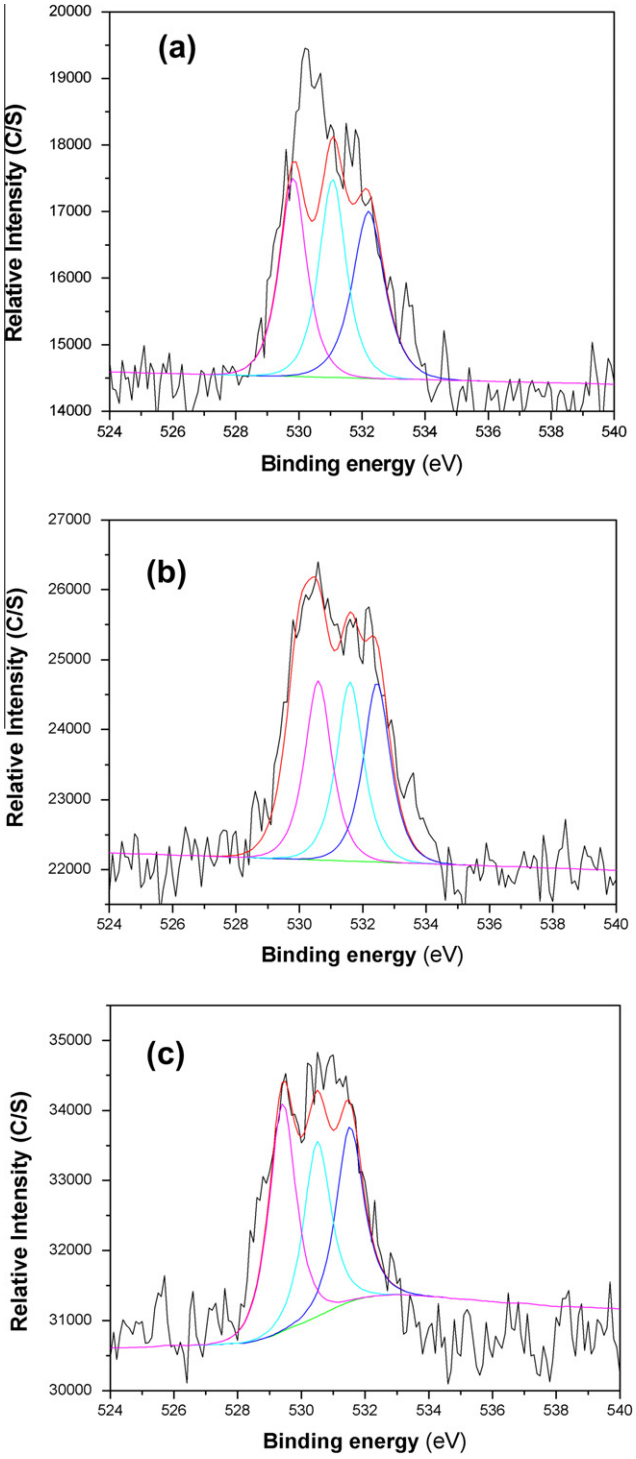

Fig. 5. Reveals the growth power influenced the oxygen bond (XPS data) of the ZnO films. (a)100 W, (b),150 W, and (c)200 W.

energetic-particle conditions at a deposition power of 200 W, relative to those obtained at 100 or 150 W, thereby enhancing the strength of the structural bonds within the ZnO films and, as a result, promoting its nanotribological properties.

4. Conclusion

We have investigated the structural features and tribological characteristics of ZnO films deposited on langasite substrates through r.f. magnetron sputtering at various deposition powers. The ZnO films possessed polycrystalline structures, with the evident (1 0 0), (0 0 2), and (1 0 1) peaks of hexagonal ZnO. As the deposition power increased, the ZnO films became predominantly oriented along the *c*-axis (0 0 2), and their surface roughness increased. It is speculated that with high RF power, the zinc atoms have more opportunity to access the substrates and increase the probability of forming nuclei, thus the growth rate of ZnO film increases with increasing RF power. The nanoscratch technique provided information regarding the near-surface friction and wear properties. The XPS-derived binding energies of the Zn and O atoms in the films suggested that the strength of the structural bonds within the ZnO films was enhanced as a result of favorable reactions of the Ar plasma during the sputtering process.

References

[1] S.A. Studenikin, N. Golego, M. Cocivera, J. Appl. Phys. 84 (1998) 2287.
[2] X.D. Li, L. Zhang, H. Gao, J. Phys. D: Appl. Phys. 37 (2004) 753.
[3] S.J. Bull, J. Phys. D: Appl. Phys. 38 (2005) R393.
[4] C.H. Chien, S.R. Jian, C.T. Wang, J.Y. Juang, J.C. Huang, Y.S. Lai, J. Phys. D: Appl. Phys. 40 (2007) 3985.
[5] V.A. Coleman, J.E. Bradby, C. Jagadish, P. Munroe, Y.W. Heo, S.J. Pearton, D.P. Norton, M. Inoue, M. Yano, Appl. Phys. Lett. 86 (2005) 203105.
[6] S. Zhao, Y. Zhou, Y. Liu, K. Zhao, S. Wang, W. Xiang, Z. Liu, P. Han, Z. Zhang, Z. Chen, H. Lu, K. Jin, B. Cheng, G. Yang, Appl. Surf. Sci. 253 (2006) 726.
[7] R. Navamathavan, K.K. Kim, D.K. Hwang, S.J. Park, T.G. Lee, G.S. Kim, J.H. Hahn, Mater. Lett. 61 (2007) 2443.
[8] S.R. Jian, I.J. Teng, P.F. Yang, Y.S. Lai, J.M. Lu, J.G. Chang, S.P. Ju, Nanoscale. Res. Lett. 3 (2008) 186.
[9] J.J. Chen, Y. Gao, F. Zeng, D.M. Li, F. Pan, Appl. Surf. Sci. 223 (2004) 318.
[10] L.Y. Lin, M.C. Jeong, D.E. Kim, J.M. Myoung, Surf. Coat. Technol. 201 (2006) 2547.
[11] H. Schulz, K.H. Thiemann, Solid State Commun. 32 (1979) 783.
[12] P.F. Yang, H.C. Wen, Y.S. Lai, C.T. Wang, S. Wu, R.S. Chen, Microelectron. Reliab. 48 (2008) 389.
[13] W.T. Lim, C.H. Lee, Thin Solid Films 353 (1999) 12.
[14] S.S. Lin, J.L. Huang, D.F. Lii, Surf. Coat. Technol. 176 (2004) 173.
[15] J.W. Shin, J.Y. Lee, T.W. Kim, Y.S. No, W.J. Cho, W.K. Choi, Appl. Phys. Lett. 88 (2006) 091911.
[16] J.M. Yuk, J.Y. Lee, J.H. Jung, T.W. Kim, D.I. Son, W.K. Choi, Appl. Phys. Lett. 90 (2007) 031907.
[17] K.B. Sundaram, A. Khan, Thin Solid Films 295 (1997) 87.
[18] Y.M. Lu, W.S. Hwang, W.Y. Liu, J.S. Yang, Mater. Chem. Phys. 72 (2001) 269.
[19] N. Almqvist, Surf. Sci. 355 (1996) 221.
[20] S.V. Prasad, S.D. Walck, J.S. Zabinski, Thin Solid Films 360 (2000) 107.
[21] Chao, S.J. Lin, W.C. Chang, Nucl. Instr. Meth. B 268 (2010) 1581.
[22] L. Shen, Z.Q. Ma, C. Shen, F. Li, Nucl. Instr. Meth. B 268 (2010) 2679.
[23] Md Nurul Islam, T.B. Ghosh, K.L. Chopra, H.N. Acharya, Thin Solid Films 280 (1996) 20.
[24] S. Komuro, T. Katsumata, T. Morikawa, X. Zhao, H. Isshiki, Y. Aoyagi, J. Appl. Phys. 88 (2000) 7129.
[25] M. Futsuhara, K. Yoshioka, O. Takai, Thin Solid Films 322 (1998) 274.
[26] Z.B. Gu, M.H. Lu, J. Wang, D. Wu, S.T. Zhang, X.K. Meng, Y.Y. Zhu, S.N. Zhu, Y.F. Chen, Appl. Phys. Lett. 88 (2006) 082111.
[27] J.B. Lee, H.J. Kim, S.G. Kim, C.S. Hwang, S.H. Hong, Y.H. Shin, N.H. Lee, Thin Solid Films 435 (2003) 179.
[28] Y.M. Lu, W.S. Hwang, W.Y. Liu, J.S. Yang, Mater. Chem. Phys. 72 (2001) 269.